ELSEVIER

Surface Science 420 (1999) 103–109

surface science

Surface relaxation of the (110) face of rutile SnO_2

Tapio T. Rantala, Tuomo S. Rantala, Vilho Lantto *

[a] *Department of Physical Sciences, University of Oulu, FIN-90570 Oulu, Finland.*
[b] *Microelectronics and Materials Physics Laboratories, University of Oulu, FIN-90570 Oulu, Finland.*

Received 22 August 1998; accepted for publication 20 October 1998

Abstract

Surface relaxation of the stoichiometric and reduced SnO_2 (110) surfaces is studied with first-principles calculations. Calculations are carried out with two different self-consistent ab initio LDA methods, which lead to similar results. The most prominent feature in the relaxation is that the surface layer oxygens of the reduced surface move outwards about 0.4 Å with respect to the surface tin atoms. The stoichiometric (oxidized) surface is stabilized by the "bridging" oxygen atoms, and therefore, relaxes less. The valence band density-of-states is similar at both surfaces, except that removing bridging oxygens leaves behind electrons that occupy gap states formed at the reduced tin atoms. © 1999 Elsevier Science B.V. All rights reserved.

Keywords: Density functional calculations; Semiconducting surfaces; Single crystal surfaces; Surface relaxation and reconstruction; Tin oxides

1. Introduction

Compound semiconductors and their specific properties of interfaces and surfaces are widely used in today's electronics. In semiconductor gas sensors, for example, the chemical signal is transduced through the electronic structure of the material to measurable electrical characteristics. Tin dioxide (SnO_2) is used in gas sensing applications because of its stability in high temperatures and environment dependent surface chemistry. The "oxygen chemistry" at the grain surfaces of the usually porous SnO_2 material is strongly dependent on the surrounding gas atmosphere and it is reflected in the easily measurable electric conductance [2]. We therefore study here the detailed structure of the most stable face (110) of the rutile structure SnO_2 to lay a background for understanding the oxygen-related surface reactions.

Extensive research has been done on the SnO_2 material and its surfaces both experimentally and theoretically. The surface electronic structure has been investigated with various spectroscopies and surface states in the band gap were found in case of the reduced surface [3]. It was concluded that they arise from the "bridging" oxygen vacancies, because these states were absent at the stoichiometric surface. The surface topology has been investigated using LEED and most recently using STM; see Ref. [4] and further references therein. Depending on the experimental conditions at least (1×1), (1×2) and (4×1) reconstructions were observed. It seems obvious, however, that the ideal reduced and stoichiometric surfaces appear in the (1×1) reconstruction. Unfortunately, there are no direct experimental data about the surface relaxation perpendicular to the (110) face.

* Fax: +358-8-553-1287;; e-mail: Tapio.Rantala@oulu.fi.

0039-6028/99/$ – see front matter © 1999 Elsevier Science B.V. All rights reserved.
PII: S0039-6028(98)00833-4

Previously, we have studied the unrelaxed SnO_2 surface computationally with density-functional theory and the local-density approximation (DFT-LDA) using cluster models and the linear combination of atomic orbitals (LCAO) method. The ideal (unrelaxed) nonpolar (110) surface was investigated with different oxygen contents [5]and other adsorbates [6]. We found in agreement with Cox et al. [3]that band gap levels arise from the "bridging" oxygen vacancies. It became apparent, however, that relaxation of the surface is essential in explaining the surface electronic structure and the finite-size cluster effects have to be eliminated in order to obtain quantitative results reliably. This motivated us now to investigate computationally the surface relaxation of the SnO_2 (110)-1×1 surface using a three-dimensional periodic slab model. The slab model was chosen, because it eliminates the finite-size effects both in the surface relaxation and electronic structure.

Bulk band structure calculations of Palummo et al. [7] proved the importance of relaxation within the LDA calculation scheme. The band gap, if first calculated with the experimental lattice geometry and crystal volume, increased by about 50% when using the relaxed geometry. Further inclusion of the self-energy correction led to a value 3.4 eV, which is close to the experimental band gap. Munnix and Schmeits calculated the electronic structures of several ideal (unrelaxed) SnO_2 surface faces using a tight-binding (TB) method [9]. They did not find any surface states in the band gap contrary to the experimental UPS observation of Cox et al. [3]. The TB calculations of Godin and LaFemina [10] did not reveal any gap states either, though they specifically calculated the surface relaxation of the SnO_2 (110)-1×1, which suggests that the relaxation is not behind the possible formation of surface gap states.

Closest to our present work comes the first-principles LDA slab calculations of Manassidis et al. [12]. They find a similar surface relaxation at both stoichiometric and reduced surfaces, which differs from our main result, as discussed below. The surface density-of-states they obtain, however, is similar to ours: they find surface states in the band gap at the reduced surface, but not at the stoichiometric surface. Goniakowski et al. [14] have investigated bulk and surface properties of SnO_2 (and TiO_2) with gradient-corrected LDA. Though they find that the gradient corrections reduce surface energies by about 30% and increase the lattice constants by a few percent, the effects on the relaxed surface structure and electronic density of states being almost negligible. On the other hand, for the adsorption energetics of water molecules on the surfaces the gradient corrections to LDA appeared to be crucial [14].

In this study we consider relaxation of two ideal (110) surfaces of SnO_2, one of which is called "reduced" and the other oxidized or "stoichiometric" surface. We present results from two independent computational approaches. One is based on the LCAO scheme and used with a frozen core approximation. The other is based on a plane wave expansion for the valence electrons and pseudopotential approximation for the atomic cores (PWPP). Both methods are based on the LDA. The use of two independent calculation schemes provides us with an additional control of method independence.

In Section 2 we describe our slab models for the stoichiometric and reduced surfaces. Then we briefly describe the computational methods in Section 3 and results will be given in Section 4. Section 5 concludes the discussion.

2. The slab model of SnO_2 – 1×1 face

A perfect SnO_2 crystal is an insulator with a direct band gap of 3.6 eV. However, the natural doping by oxygen vacancies renders it an n-type semiconductor. The rutile crystal structure of SnO_2 is 6:3 coordinated and the bonding between atoms has a relatively strong ionic character. The tetragonal unit cell contains two tin and four oxygen atoms with the experimental lattice parameters $a = 4.737$ and $c = 3.186$ Å, see Fig. 1a. The direction of the structure consists of neutral groups of three parallel planes O–Sn_2O_2–O and the cleavage cut between these groups of planes breaks the least number of cation–anion bonds. This results in what is called the stoichiometric surface. Therefore, the (110) face is the most stable and

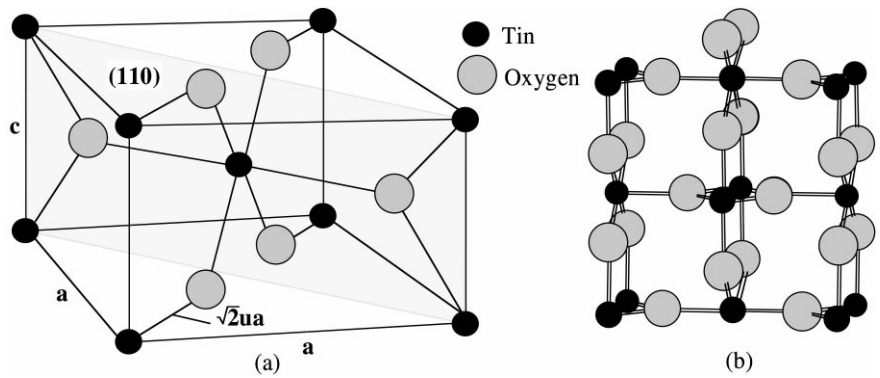

Fig. 1. (a) The primitive tetragonal unit cell of the bulk SnO_2, with the basis $(SnO_2)_2$. The lattice parameters are $a=4.737$ Å, $c=3.186$ Å and $u=0.306$. (b) The orthorhombic supercell of rutile SnO_2 used in the thinnest slab model. The top face of the supercell illustrates the stoichiometric and the bottom face the reduced (110) surface. In calculations, however, both surfaces were either stoichiometric or reduced. The volume (6.70 Å × 3.19 Å × 6.70 Å) of the supercell shown is twice that of the bulk primitive cell. In the slab supercell [6.70 Å × 3.19 Å × (6.70 + vacuum) Å] there are 6 Sn and 10 O atoms (reduced) or 6 Sn and 12 O atoms (stoichiometric).

most dominant surface of the crystallites of the usually porous SnO_2 material. Removal of the surfacemost "bridging" oxygen layer of the stoichiometric surface results in what is called the reduced (110) surface.

To form the slab model of the (110) surface we use an orthorhombic supercell with 16 atoms (reduced, Sn_6O_{10}) or 18 atoms (stoichiometric, $(SnO_2)_6$) oriented as shown in Fig. 1b. The vacuum between the surfaces was chosen to occupy half of the slab supercell. In addition to the minimum slab thickness (6.70 + 6.70 Å) with LCAO we also calculated the double size of that (13.40 + 13.40 Å). All atoms except for those in the innermost atomic plane were allowed to relax in the smaller (thinner) slab and one more atomic plane in the double sized slab, i.e. three or four planes (at both sides) plus the possible bridging oxygens, respectively. The upper and lower sides were treated identically but the centermost plane(s) were kept fixed.

Bates et al. [15] have carried out a systematic study of the slab model for the DFT–GGA calculations of the rutile surface, TiO_2 (110). They find that at least a six-layer slab with 4 Å vacuum is needed for the convergence of surface energy but less is sufficient for the calculation of surface atomic structure. Therefore, we expect our slab model to be sufficiently large. Furthermore, according to our experience with SnO_2 the slab thickness convergence depends on the number of atomic planes allowed to relax.

3. Computational methods

One of our computational tools, DSolid, is a commercially distributed software [16]. It allows self-consistent computation of periodic structures within the LCAO (linear-combination-of-atomic-orbitals), i.e. a localized basis set, and DFT (density-functional theory). The basis functions are one-electron orbitals of free atoms and free ions computed and stored in a numerical form prior to the crystal (slab) calculation. The typical extent of radial functions is 5–6 Å. This type of basis allows one to use high quality but relatively small basis. Thus, for oxygen and tin we used the basis sets: $1s^2$, $2s^2$, $2p^4$, $2s^{0*}$, $2p^{0*}$, $3d^{0*}$, $3d^{0*}$, and $(1s^2)$, $(2s^2)$, $(2p^6)$, $(3s^2)$, $(3p^6)$, $(3d^{10})$, $(4s^2)$, $(4p^6)$, $4d^{10}$, $5s^2$, $5p^2$, $4d^{0*}$, $5s^{0*}$, $5p^{0*}$, $5d^{0*}$, respectively. The basis functions in parentheses represent the "frozen core" and those marked with an asterisk were generated in ions rather than in neutral atoms. For the exchange and correlation within DFT we restricted ourselves to the LDA (local-density approximation) and used the parametrizations of Janak et al. [16], and Vosko et al. [17] , which both led to similar results.

The supercell of the slab model was used as a computational unit cell. In the present method periodic boundary conditions are invoked simply by summing up the one-electron wave functions formed from the localized basis functions at the atomic sites throughout the whole periodic system. If compared with the plane wave method below, this kind of "embedding" corresponds to incorporation of one **k**-point Γ, only, and is therefore called a Γ-point approximation. The quality of this approximation was tested by doubling the size of the computational unit cell in two different coordinate directions.

The other computational tool, PlaneWave, is based on the pseudopotential (PP) description of ion cores and a plane wave expansion for the valence and conduction electrons (PWPP) [16]. The pseudopotentials were chosen to be of extended-norm-and-hardness-conserving type [18] after careful testing. The softer norm-conserving pseudopotentials of Troullier and Martins [19] were found to lead to incorrect bulk lattice constants. The chosen pseudopotentials replace the core orbitals O: $1s^2$ ($l=0$, 1) and Sn: ($1s^2$), ($2s^2$), ($2p^6$), ($3s^2$), ($3p^6$), ($3d^{10}$) ($l=$ 0–3), where the angular momentum quantum numbers l define the "non-locality". The chosen hard pseudopotentials made it necessary to use an unusually large plane wave basis, up to the cut-off of 40 Hartrees (80 Ry). The number of **k**-points was three, chosen according to the Monkhorst–Pack method [20] to optimally span the integration mesh over the Brillouin zone. An increase in the number of **k**-points had no effect on the bulk SnO_2 relaxation.

4. Surface relaxation and density of states

We first examined the bulk SnO_2 relaxation within our calculation schemes. Total energy minimization starting from the experimental lattice constants with the LCAO method led to about 3% isotropic expansion, whereas the PWPP gave only less than 0.5% expansion with the "extended-norm-and-hardness-conserving" pseudopotentials [18]. It is interesting to note that Manassidis et al. [11,12]found with a similar PWPP method a lattice shrinkage of about 3%. To retain comparability in the further surface calculations we kept the experimental lattice parameters but allowed relaxation the of atomic positions within the bulk unit cell. The atomic positions relaxed negligibly with PWPP but with the LCAO the oxygen atoms moved, but less than 0.05 Å with the relaxation energy of 0.3 eV per $(SnO_2)_4$ unit cell.

With the experimental lattice constants but bulk relaxed initial atomic positions the surface relaxation energies per surface unit cell were found to be 0.15 and 1.0 eV with the LCAO, and 0.4 and 0.5 eV with the PWPP, for the stoichiometric and reduced surfaces, respectively. These can be compared with the 0.5–0.6 eV relaxation obtained by Manassidis et al. [11,12] for the stoichiometric surface with PWPP.

Both surfaces relaxed without reconstructions preserving their truncated bulk symmetry properties. The parameters used to describe the relaxation are introduced in Fig. 2 and their calculated values are given in Table 1. There are no experimental values to compare with, but instead, we give the calculated values of Manassidis et al. (PWPP), and Godin and LaFemina (TB) .

The most prominent feature is that the surface layer oxygens relax outwards with respect to 5-fold tin atoms ($\Delta_{1\perp 2}$). This is true for all calculations and only the extent of relaxation varies. We find this to be strong (≈ 0.4 Å) for the reduced surface and less for the stoichiometric surface. This difference is made even stronger by the 5-fold tin atom relaxation outwards ($d_{12\perp}$) in the reduced surface. The relative displacements of the surface layer tin atoms $\Delta_{1\perp 1}$ do not differ essentially at the two surfaces, and thus, the reduced surface layer tin atoms, in average, have moved out more prominently, cf. $d_{12\perp}$ and $d_{12\perp}+\Delta_{1\perp 1}$.

The subsurface oxygens and 4- or 6-fold tin atoms above them have the same relative displacement $\Delta_{1\perp 4}+\Delta_{1\perp 1}\approx 1.4$ Å at both surfaces. Finally, the case of bridging oxygens is interesting. Though they come slightly closer to the 6-fold tin atoms ($\Delta_{1\perp 3}-\Delta_{1\perp 1}$), the net relaxation is clearly out from the surface ($\Delta_{1\perp 3}$). This is quite different from the relaxation of the stoichiometric $TiO_2(110)$ surface (same topology), where the bridging oxygens have been experimentally observed to relax strongly into

Fig. 2. The relaxation parameters of SnO_2 surface as defined in Ref. [10], cf. the orthorhombic unit cell in Fig. 1b. (a) Top view and (b) side view.

Table 1
The relaxation parameters of the SnO_2 (110) surface as defined in Fig. 2 (all values are in Å). For LCAO the values are given for the double size slab, only, as the differences with the thinner slab do not exceed 0.02 Å. The "unrelaxed" column shows the experimental values for the truncated bulk geometry. The unrelaxed reference for each of the calculations is the calculated bulk relaxed geometry, and thus, different for each of the columns

Parameter	Unrelaxed	LCAO	PWPP	PWPP [11,12]	TB [10]
Stoichiometric		$Sn_{10}O_{20}$	Sn_6O_{12}	Sn_8O_{16}	
$\Delta_{1\perp1}$	0	+0.08	+0.21	+0.30	+0.10
$\Delta_{1\perp2}$	0	+0.04	+0.22	+0.22	+0.29
$\Delta_{1\perp3}$	1.29	1.36	1.41	1.46	1.37
$\Delta_{1\perp4}$	1.29	1.36	1.22		1.18
Δ_{1y}	2.59	2.63	2.50		2.53
Δ_{2y}	2.59	2.71			2.57
$d_{12\perp}$	3.35	3.33	3.26		3.24
$\Delta_{2\perp1}$	0	−0.01			−0.08
$\Delta_{2\perp2}$	0	+0.01			+0.00
$\Delta_{2\perp3}$	1.29	1.35	1.28		1.20
Reduced		$Sn_{10}O_{18}$	Sn_6O_{10}	Sn_8O_{14}	
$\Delta_{1\perp1}$	0	+0.05	+0.11	+0.41	−0.05
$\Delta_{1\perp2}$	0	+0.45	+0.40	+0.26	+0.28
$\Delta_{1\perp4}$	1.29	1.39	1.33		1.29
Δ_{1y}	2.59	2.70	2.45		2.58
Δ_{2y}	2.59	2.71			2.57
$d_{12\perp}$	3.35	3.45	3.41		3.35
$\Delta_{2\perp1}$	0	+0.01			+0.03
$\Delta_{2\perp2}$	0	+0.00			+0.08
$\Delta_{2\perp3}$	1.29	1.41	1.36		1.31

the surface but calculations similar to those above show essentially no relaxation at all [15].

As seen above, both of our methods predict similar perpendicular relaxation for the reduced surface and the differences in predictions for the stoichiometric face are small. However, there is a

clear difference in the lateral relaxation of surface oxygens, which probably originates from the remaining strain in the bulk structure due to the use of experimental lattice constants in the LCAO approach. The largest differences between the results from our two methods are found for the lateral displacement of surface oxygens (Δ_{1y}). This, however, to large extent results from the bulk relaxation and not surface relaxation alone. Thus, it is possibly a consequence of the strain due to unrelaxed lattice constants.

As noted in Table 1, there is less than 0.02 Å difference in the atomic displacements of the three- and five-layer slabs in LCAO calculation. Thus, the slab size effects that we find are smaller than those found for the TiO_2(110) surface [15].

The PWPP results from our calculations and from those of Manassidis et al. [11,12]could have been expected to be more alike than they appear. There are no essential differences in slab structures (3 and 5 layers vs. 2 and 4 layers (top face relaxing, only)), cut-off energy (40 H vs. 37 H) or number of **k**-points (3 vs. 4). There are differences, however, in the slab model and treatment of Sn 4d electrons, and the pseudopotentials are not the same. We allow relaxation of the slab at both sides, which may have a marked effect, in particular, if dipole surface layers are involved [14]. We treat the Sn 4d cores explicitly, whereas Manassidis et al. use pseudopotentials instead. A reflection of these differences may be seen already in the different bulk relaxation that we find. Manassidis et al. find 3% contraction of the lattice whereas our PWPP calculation leads to 0.5% expansion from the experimental lattice parameters. This might also explain the similarity of the results from our two different methods, as they both tend to expand the crystal volume in bulk total energy minimization. The fact that we used the experimental lattice constants, not the bulk relaxed constants as Manassidis et al. did, may also explain part of the deviations in the calculated structures. On the other hand, the lattice constants would relax quite differently, +3% and +0.5% with the LCAO and PWPP, respectively, but nevertheless, our calculated surface relaxations with unrelaxed bulk lattice constants are very similar. Therefore, the remaining "bulk strain" cannot be responsible for much of the differences between the results of Manassidis et al. and ours.

The surface electronic structure description in terms of bands is not too complete with only the few **k**-points we use: one in LCAO or three in PWPP. Furthermore, the band gap is known to be poorly described with DFT-LDA, e.g. the bulk value for SnO_2 is around 2.2 eV [7,11,12], which is only some 60% of the experimental value. In Fig. 3 we present the densities-of-states (DOS) of the two surfaces and bulk obtained from the one-electron eigenvalues at the three **k**-points of our PWPP calculations. Note that as both sides of the slab are allowed to relax there are no one-electron eigenstates from the "truncated bulk" surface. The general shapes in various cases are in good agreement with the DOS distributions of Manassidis et al. [11,12]. The bulk valence band width is less than 8 eV and compares well with the experimental 7.5 eV. For surfaces it is somewhat larger, about 9–10 eV.

It is seen that in case of the reduced surface gap states appear as a result of removing the bridging oxygens. With the analysis of the corresponding LCAO one-electron orbitals we are able to trace their localization back to the surface tin atoms and oxygen atoms below the missing bridging oxygen sites. This supports the picture that the electrons left behind from the removed oxygens

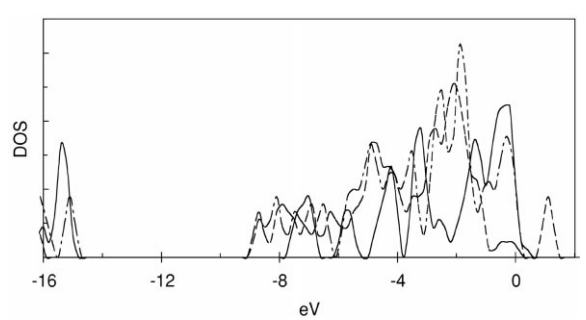

Fig. 3. The density-of-states (DOS) of the SnO_2 bulk (solid curve) and the two surfaces, reduced (dashed) and stoichiometric (dot-dashed). The distributions are approximated from the discrete spectrum of the PWPP one-electron levels by broadening of about 0.5 eV. The calculated bulk DOS is shifted downwards by 3.5 eV to match the surface DOS distributions (which are not shifted relative to each other). Only the occupied DOS is shown here.

occupy the gap states formed at the reduced surface tin atoms. The gap states form a band with relatively strong dispersion in the direction of the *c*-axis. Description of such bands requires more **k**-points or corresponding extension of the unit cell in the LCAO approach, e.g. doubling of the unit cell size in *c*-direction.

5. Conclusions

As expected, the relaxation of the (110) surface of SnO_2 occurs essentially in the perpendicular direction, only. In-plane relaxation is negligible and symmetry breaking reconstruction was not found. The most prominent feature is the surface layer anion relaxation outwards with respect to surface layer cations at the reduced surface. This appears to be strong at the reduced surface, about 0.4 Å, but much weaker at the oxidized surface. This is where our results differ from other recent ab initio calculations [11,12]. The difference may arise from the differences in slab relaxation model, pseudopotentials or treatment of Sn 4d electrons, which we include explicitly. Our two methods, LCAO and PWPP, though different in nature, lead to similar surface relaxation.

However, in an agreement with the results of Manassidis et al. [11,12]and experimental observations [3] surface gap states were found at the reduced but not at the stoichiometric surface. Also the interpretation of the origin of gap states is similar to the previous ones: the electrons released from the bridging oxygen vacancies reduce the surface layer tin atoms and form these states.

The extent of relaxation and the consequent effects on the surface properties are expected to be essential for the adsorption of oxygen and other guest molecules, and therefore, for surface chemistry of SnO_2, which will be the subject of our further studies.

Acknowledgements

The authors acknowledge the Academy of Finland for funding within the projects nr. 29261, 37778 and 37781 (MECA). The Center for Scientific Computing (CSC) at Espoo, Finland is acknowledged for providing us with the computational resources within the project number oy1199.

References

[1] V. Lantto, in: G. Sberveglieri (Ed.), Gas Sensors, Kluwer, Dordrecht, 1993, pp. 43–88.
[2] V. Lantto, V. Golovanov, Sensors and Actuators B 24–25 (1995) 614.
[3] D.F. Cox et al., Phys. Rev. B 38 (1988) 2072.
[4] F.H. Jones et al., Surf. Sci. 376 (1997) 367.
[5] T.S. Rantala, V. Lantto, T.T. Rantala, Sensors and Actuators 18–19 (1994) 716.
[6] T.S. Rantala, V. Lantto, T.T. Rantala, Physica Scripta T54 (1994) 252.
[7] M. Palummo et al., in: Proc. 22nd Int. Conf. on the Physics of Semiconductors, 1995, pp. 161–164.
[8] S. Munnix, M. Schmeits, Phys. Rev. B 27 (1983) 7624.
[9] S. Munnix, M. Schmeits, Phys. Rev. B 33 (1986) 4136.
[10] T.J. Godin, J.P. LaFemina, Phys. Rev. B 47 (1993) 6518.
[11] I.. Manassidis et a, Surf. Sci. 339 (1995) 258.
[12] I. Manassidis, M.J. Gillan, Surf. Rev. Lett 1 (1994) 491.
[13] J. Goniakowski et al., Phys. Rev. B 53 (1996) 957.
[14] J. Goniakowski et al., Surf. Sci. 350 (1996) 145.
[15] J.P. Bates et al., Surf. Sci. 385 (1997) 286.
[16] User Guides of DSolid and PlaneWave, Molecular Simulations, San Diego, CA, 1996.
[17] S.H. Vosko, L. Wilk, M. Nusair, Can. J. Phys. 58 (1980) 1200.
[18] M.P. Teter, Phys. Rev. B 48 (1993) 5031.
[19] N. Troullier, J.L. Martins, Solid State Commun. 74 (1990) 613.
[20] H.J. Monkhorst, J.D. Pack, Phys. Rev. B 13 (1976) 5188.